POLITECNICO DI TORINO
Repository ISTITUZIONALE

Transient formation of the passive scalar spectrum at a turbulent interface

Original
Transient formation of the passive scalar spectrum at a turbulent interface / DI SAVINO, Silvio; Gallana, Luca; Iovieno, Michele; Tordella, Daniela. - (2013), pp. 38-38+CD(1-10). (Intervento presentato al convegno XXI Congresso AIMETA tenutosi a Torino nel 17-20 settembre 2013).

Availability:
This version is available at: 11583/2518628 since:

Publisher:
Edizioni Cortina

Published
DOI:

Terms of use:

This article is made available under terms and conditions as specified in the corresponding bibliographic description in the repository

Publisher copyright

(Article begins on next page)

25 April 2024

Transient formation of the passive scalar spectrum at a turbulent interface

Michele Iovieno[1], Silvio Di Savino[1], Luca Gallana[1], Daniela Tordella[1]
[1]*Dipartimento di Ingegneria Meccanica e Aerospaziale, Politecnico di Torino, Italy*
E-mail: michele.iovieno@polito.it

Keywords: turbulence, mixing, passive scalar.

SUMMARY. The transport of a passive scalar through turbulent-turbulent interface between two decaying isotropic turbulent flows with different kinetic energy is investigated in both two and three dimensions by means of direct numerical simulations. A high scalar variance region is generated at the initial interface and two intermittent fronts appear at the borders of this zone. These fronts propagate toward the homogeneous regions in both the direction of the passive scalar flow and the opposite direction. In the central part of the mixing layer, between these two intermittent fronts, the spectrum of the scalar fluctuations shows a full range of scales just after one eddy turnover time, with a more prominent inertial range region than the velocity spectrum. This feature is preserved for about ten eddy turnover times, during which the scalar variance slowly reduces as the turbulence decays.

1 INTRODUCTION

The advection of a passive substance by a turbulent flow is important in many natural and engineering contexts, e.g. turbulent mixing, combustion, pollution dispersal, in which the prediction of mixing and dispersion rates of a passive scalar contaminant is a problem of great interest because of the concern over the design of efficient mixing and combustion devices and over environmental emissions. Although the concentration of such a passive substance exhibits a complex behaviour that shows many phenomenological parallels with the behaviour of the turbulent velocity field, the statistical properties of 'passive scalar' turbulence, strongly influenced by the Kolmogorov cascade phenomenology, are in part decoupled from those of the underlying velocity field, [1].

The subject, in the last years, is in fact undergoing a reinterpretation as empirical evidence shows that local isotropy, both at the inertial and dissipation scales, is violated [2]. Moreover in practice, dispersion usually occurs in time dependent inhomogeneous flows, which present a much more complicate behaviour than homogeneous flows and thus are beyond the reach of analytical models or even numerical simulations. In this work, we go one step beyond the homogeneous and isotropic turbulence and consider the simplest inhomogeneous and shearfree turbulent Navier-Stokes motion: The system here considered is characterized by one energetic turbulent isotropic field that is left to convectively diffuse into a low energy one. In this system the region where the two turbulences interact is preceded by a highly intermittent thin layer - where the energy flux is maximum - that propagates into the low energy region, see [3, 4]. The presence of the interaction zone offers the way to carry out numerical measurements of the long-term temporal turbulent diffusivity in an inhomogeneous flow. Moreover, we can see how scalar fluctuations and their spectra evolve in time in this inhomogeneous flow.

The initial condition construction and computational method are described in section 2. In section 3, we present new results concerning the passive scalar turbulent transport in two and three dimensions, which comprehend the first four moments of the passive scalar concentration, the skewness and kurtosis of the passive scalar derivative and the passive scalar spectra.

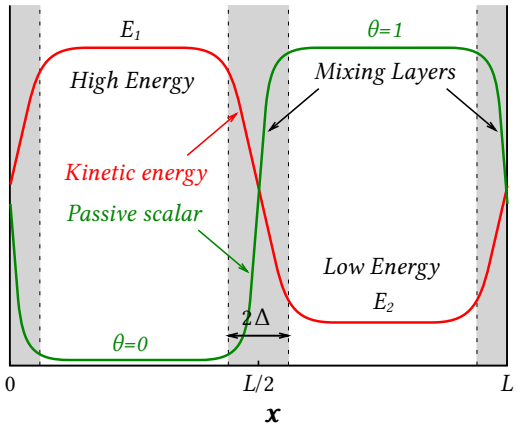

Figure 1: Scheme of the flow. Due to the use of periodic boundary conditions, two interfaces are included in the computational domain along the x direction, which is the direction where the inhomogeneity takes places. The flow is homogeneous in the other two direction,s y_1 and y_2, not shown in the sketch. L is the domain size in x direction. The initial conditions for the velocity are generated by a linear matching of two homogeneous and isotropic fields over a thickness Δ, see equation (2), while the initial mean scalar distribution is a discontinuity smoothed enough to avoid the Gibbs phenomenon, see equation (3).

2 METHOD

We numerically solve the Navier Stokes equations for an incompressible fluid together with the advection-diffusion equation for a passive scalar,

$$\frac{\partial \theta}{\partial t} + u_j \frac{\partial \theta}{\partial x_j} = \kappa \nabla^2 \theta \tag{1}$$

where κ is the diffusivity of the passive scalar. Figure 1 shows a schematic diagram of the flow configuration and the coordinate system used. The flow is assumed to be contained in a parallelepiped (or a rectangle in two dimensions) and periodic boundary conditions are applied to all the spatial directions. In the initial condition, two isotropic turbulent fields are separated by a thin layer which is as thick as the correlation length ℓ. The coordinate system is chosen with the x axis along the direction of the energy gradient, axis y_1 and y_2 along the homogeneous directions. The initial condition is obtained by matching two homogeneous and isotropic fields with the same integral scale but with a different turbulent kinetic energy as in [3, 4]. In practice, the initial condition is generated as $u_i = u_i^{(1)} p(x)^{\frac{1}{2}} + u_i^{(2)} (1-p(x))^{\frac{1}{2}}$, where $u_i^{(1)}$ and $u_i^{(2)}$ are the velocity of two homogeneous and isotropic fields with turbulent kinetic energies equal to E_1 and E_2. The weighting function $p(x)$, defined as

$$p(x) = \frac{1}{2}\left[1 + \tanh a\frac{x}{L} \tanh a\frac{x - L/2}{L} \tanh a\frac{x-L}{L}\right], \tag{2}$$

have been chosen to allow a smooth transition between the two regions (in eq. 2 L is the domain size in the x direction and a is a constant, which is chosen in order to have an initial transition layer that is no larger than the integral scale, $a = 55$). In this study, $u_i^{(2)} = u_i^{(1)}/\mathcal{E}^{1/2}$, where $\mathcal{E} = E_1/E_2$ is

the imposed initial energy ratio and the two regions have the same integral scale. A description of the possible enhancement or damping of the turbulent diffusion and interface penetration associated to the presence of different integral scale can be found in [3].

In order to analyse the diffusion of the passive scalar interface across the kinetic energy gradient, the passive scalar is introduced in the low energy region of the flow at $t = 0$. To avoid the Gibbs phenomenon, the discontinuity is replaced by a smooth transition. The initial condition for the passive scalar θ is thus defined as

$$\theta(x, y_i) = \frac{1}{2}\left[1 - \tanh 2a\frac{x}{L}\tanh 2a\frac{x - L/2}{L}\tanh 2a\frac{x - L}{L}\right], \tag{3}$$

By choosing $a = 55$ in eq. (3), the scalar interface is smoothed on a length which is about half the initial integral scale. No scalar fluctuation is introduced: the scalar concentration is initially uniform in the two isotropic regions, $\theta = 0$ in the high energy region and $\theta = 1$ in the low energy region. Scalar variance will be generated by the underlying turbulent flow, as it will be shown in next section. The mass, momentum and and the scalar transport equation are solved by using a dealiased pseudospectral Fourier-Galerkin spatial discretization coupled with a fourth order Runge-Kutta explicit time integration [5].

We have carried out a numerical experiments with an imposed initial energy ratio of 6.7 in both two and three dimensions. In the three-dimensional simulations, we have performed two experiments in which the higher energy turbulent field $u_i^{(1)}$ has a Taylor microscale Reynolds number equal to 150 and 250. The Schmidt number $Sc = \kappa/nu$ is assumed to be equal to one in all the simulations.

The size of the dimensionless computational domain is $4\pi \times (2\pi)^2$ in the three-dimensional simulations. It is discretized with 1200×600^2 grid points in the simulation at $Re_\lambda = 150$ and with 2048×1024^2 in the simulation at $Re_\lambda = 250$. The domain used in the two-dimensional simulation has the same aspect ratio: it is $4\pi \times 2\pi$ and is discretized with 4096×2048 grid points. For further details on the initial conditions generation, see [3, 6].

About 20 initial eddy turnover times have been simulated in two dimensions and ten initial eddy turnover times in three dimensions. It has been estimated that the mixing layer growth will destroy the two separate homogeneous and isotropic regions after after about 30-35 initial eddy turnover times. Directions y_1 and y_2 in this flow configuration remain statistically homogeneous during the decay, so that all the statistics can be computed as plane averages in these directions. Moreover, in two dimensions the simulation has been repeated fifty times with different but statistically equivalent random initial conditions in order to enlarge the statistical sample.

3 RESULTS

The initial conditions for the velocity field introduce a kinetic energy gradient in the direction of inhomogeneity x which produces a mixing region as already shown in many experiments (e.g. [7, 3, 9]). Outside this inhomogeneous region, the kinetic energy shows a power law decay, with exponent approximately equal to -1.2, in three dimensions, while the two-dimensional flow does not present any significant energy decay.

As it has already been observed, the energy mixing layer becomes highly intermittent and the velocity fluctuations in the x direction have large skewness and kurtosis, see [3, 4, 7], with a peak shifted toward the lower energy flow. Across the mixing the second, third and fourth velocity moments collapse using a single lengthscale, the mixing width Δ_E, conventionally defined as the distance between the points with normalized energy $(E(x,t) - E_2(t))/(E_1(t) - E_2(t))$ equal to 0.75 and 0.25. A detailed description of the velocity statistics can be read in the above mentioned papers;

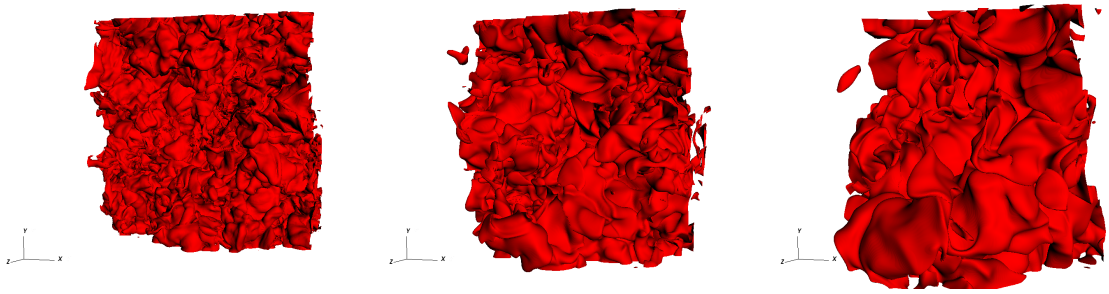

Figure 2: Visualization of the interface: isosurface $\theta = 0.1$ of the scalar field in three different instants, three dimensional mixing with $Re_\lambda = 250$. The low energy turbulence is on the left of each image. The three different instants correspond, from left to right, to $t/\tau = 1, 4, 8$, where τ is the initial eddy turnover time of the high energy region. Only one quarter of the computational domain is shown.

in this work, we focus on the passive scalar transport.

The passive scalar interface, which initially separates the low energy region with passive scalar concentration $\theta = 1$ from the high energy region with passive scalar concentration $\theta = 0$, is spread by turbulent eddies, see figure 2, and a passive scalar mixing region with high passive scalar variance is generated. The width of this region can be measured by considering the mean passive scalar distributions (figure 3(a,b)): the scalar thickness Δ_θ is defined, in analogy with the energy layer thickness Δ_E, as the distance between the points with means passive scalar $\overline{\theta}$ equal to 0.75 and 0.25. After an initial transient of about one eddy-turnover time, the time evolutions of these interaction widths closely follow those observed for the self-diffusion of the velocity field with the same dimensionality, and a stage of evolution with a power law scaling of the mixing thickness is reached in both two and three dimensions. However, the time scaling of the growth of the interaction width is superdiffusive in two dimensions ($\Delta_\theta \sim t^{0.7}$), while it is very slightly subdiffusive in three dimensions ($\Delta_\theta \sim t^{0.46}$ at $Re_\lambda = 150$ and $\Delta_\theta \sim t^{0.5}$ at $Re_\lambda = 250$), see figure 3(c,d). The same mixing length growth can be observed in the absence of the kinetic energy gradient (that is, $E_1/E_2 = 1$) and thus does not seem to be influenced by the presence of the energy gradient.

The observed growth rates are, for the three dimensional flow, in fair agreement with the wind tunnel experiments on the scalar diffusion from a linear source in a shearless mixing [7, 8], even if the long time $t^{0.34}$ suggested scaling was not observed.

In the three-dimensional flow, the passive scalar variance has already reached its maximum after less than one eddy turnover time and, since that instant, it slowly decreases. In the following 10 eddy turnover times, about 20% of the variance are $t/\tau = 1$ is lost. In two dimensions, the passive scalar flow is almost twice as large and the initial variance generation last longer: the maximum is attained later and is about 50% higher. Notwithstanding the presence of the energy gradient, the mean passive scalar and passive scalar variance profiles are almost symmetric, see figures 3 and 4. The presence of the turbulent energy gradient is instead felt on the higher order moments.

In contrast with the velocity skewness, the spatial distribution of the scalar skewness shows the presence of two intermittent fronts at the borders of the mixed region. In three dimensions, these fronts are located at a distance from the initial interface which is approximatively equal to $2\Delta_\theta$. The asymmetry in their position and in their intermittency levels is mild and tend to be less pronounced

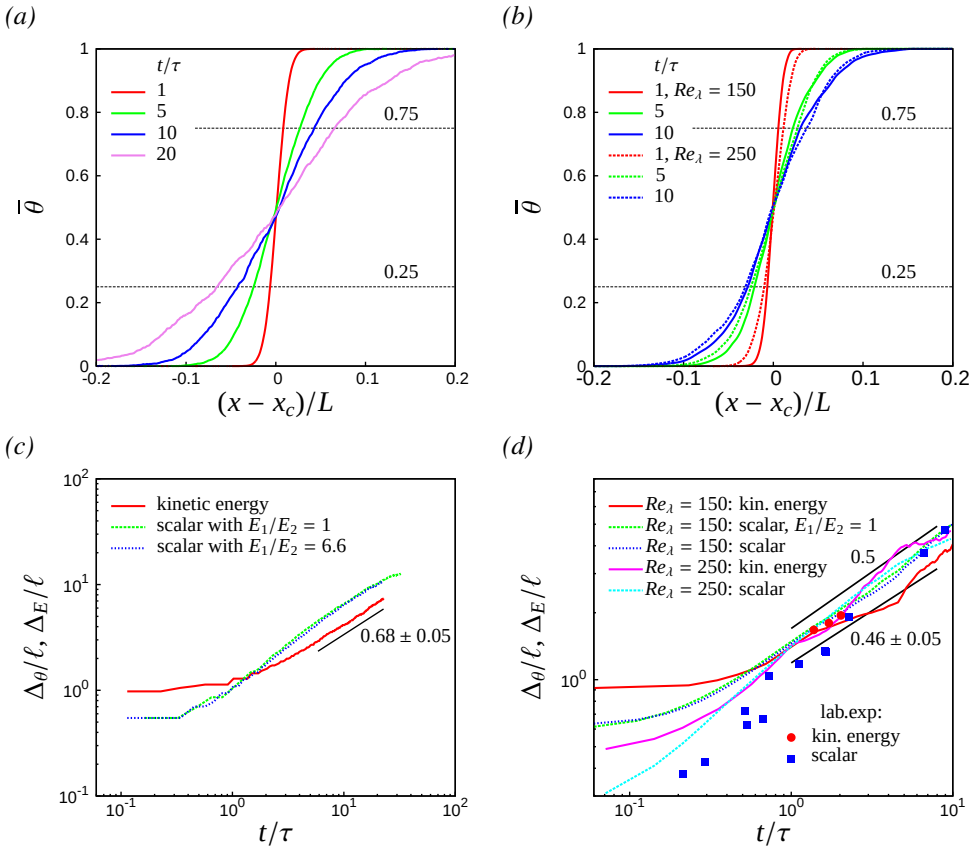

Figure 3: Mean scalar profiles inside the mixing layer: (a) two dimensional flow, (b) three dimensional flow. The initial energy ratio E_1/E_2 is equal to 6.7 in both cases. L is the domain size in the x direction and x_c the centre of the mixing layer. Interaction layer thickness, normalized with the initial integral scale ℓ: (c) two dimensional flow, (d) three dimensional flow. The scalar layer thickness Δ_θ is defined as the distance between the points where $\overline{\theta}$ is equal to 0.25 and 0.75. The energy layer thickness is defined as the distance between the points where the normalized turbulent kinetic energy $(E - E_2)/(E_1 - E_2)$ is equal to 0.25 and 0.75 as in [4]. The exponents of the power law fitting of the scalar thickness growth are indicated. The accuracy of the exponents is about 10%. Experimental data are from the wind tunnel experiments by [7] and [8] with $E_1/E_2 = 7$.

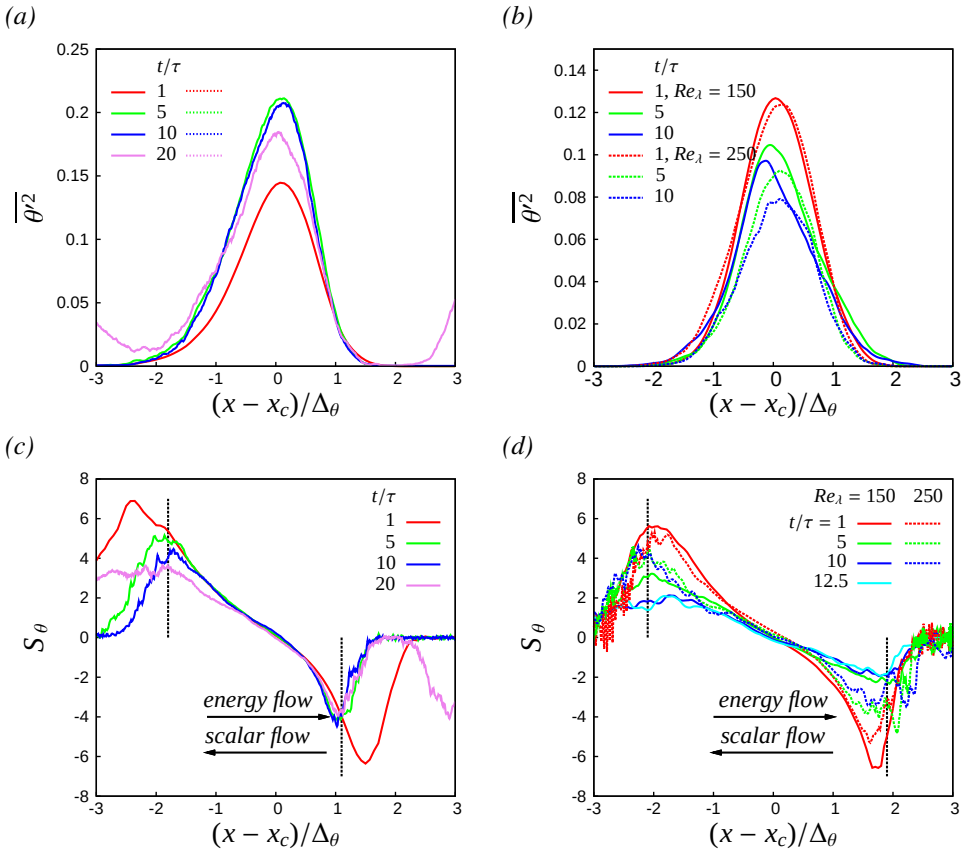

Figure 4: (a) Scalar variance distribution in two dimensional flow, (b) Scalar variance distribution in three dimensional flow. (c) Passive scalar skewness distribution in two dimensions, (d) Passive scalar skewness distribution in three dimensions. In all simulations the energy ratio is equal to 6.7 and the energy flow is from left to right.

as the mixing proceeds. On the contrary, in two dimensions the front toward the high energy regions penetrates much more than the one toward the low energy region: after about 5 initial eddy turnover times the depth of penetration is about $2\Delta_\theta$ in the high energy region and about Δ_θ in the low energy region, see figure 4(c,d). Because of the gradual thickening of the mixing layer, the kinetic energy and the passive scalar gradients, which drive the passive scalar spreading, become milder and milder. As a consequence, not only the passive scalar flux is reduced but also the intermittency levels of the two passive scalar fronts decrease in time, even if in a slower fashion. This is more evident in three dimensions where also the decay of the energy contributes to reduce the scalar variance production and the intermittency. In fact, comparing the two and three dimensional flow, the peaks in the distributions of skewness are similar after about one eddy turnover times but, after ten eddy turnover times, the peaks of skewness are twice as high in the two dimensional flow.

The skewness obtained from present simulations can be compared with the results present in the literature. For example, Donzis and Yeung [13] found a passive scalar skewness between 1.39 ($Re_\lambda = 140$) and 1.34 ($Re_\lambda = 240$) in a simulation of an isotropic turbulence with a uniform mean scalar gradient. We have obtained a much higher passive scalar skewness which, in the first five eddy turnover times, is between 3 and 5.5 at $Re_\lambda = 150$ and between 4 and 5.7 at $Re_\lambda = 250$.
Both the Reynolds number and the energy gradient influence the intermittency of the passive scalar field, and a proportional dependence between Reynolds number and intermittency has been found, for example, by Emran and Schumacher in a numerical simulation of Rayleigh-Bernard convection [16]. Schumacher found, in a direct numerical simulation of the mixing of the passive scalar at moderate Reynolds number, that the probability density function of the magnitude of the passive scalar gradient increase as Reynolds number increases[15]: a larger Reynolds number enables the passive scalar to be more efficiently stirred on all scales leading to an increase of scalar fluctuations and derivative moments. However, in this shearless flow, the energy gradient, identical at both Reynolds number, seems to overshadow the Reynolds number dependence.

Simulations in absence of an energy gradient (i.e., $E_1/E_2 = 1$), not shown in the figures, do not show this asymmetry in the position of the two two passive scalar intermittent fronts at the borders of the mixed layer even if the passive scalar thickness follows the same temporal growth.

In the central part of the mixing layer, between the two intermittent fronts, the passive scalar fluctuations tend, after few eddy turnover times, to an almost steady state: as shown in figure 4(a,b), the variance in the centre of the mixing region varies very slowly even in the three-dimensional flow, which has a relevant kinetic energy decay of the underlying flow (see [4]). Figure 5 shows the compensated one-dimensional passive scalar spectra in the centre of the mixing layer. A full range of scales is present just after one eddy turnover time. The spectra in figure 5 have been compensated by their inertial range exponents. In three dimensions, the inertial range scaling $\kappa^{-5/3}$ has been used, [17]. In two dimensions, the fitting of the data gives an the inertial range exponent equal to about -1.4. This exponent is roughly one half of the -3 exponent of the velocity field and is far from the κ^{-1} inertial range scaling of homogeneous and statistically stationary flows (see, e.g., [12],[14]). The difference between passive scalar and velocity exponents is very mild in three dimensions as both tend to approach the Kolmogorov homogeneous turbulence scaling: at $Re_\lambda = 250$ we have computed an inertial range exponents equal to 1.5 (velocity spcetrum) and 1.62 (passive scalar spectrum). The velocity spectrum inertial scaling exponent is slightly lower than the one of the passive scalar field, in agreement with the prediction by [10] – which would give 1.58 and 1.62 respectively at $Re_\lambda = 250$ – and with similar findings in different flows (see, e.g., [18]). Moreover, the passive scalar spectrum seems to show a wider inertial range region, a feature which has been observed also in homogeneous flows at moderate Reynolds numbers, see [10, 11].

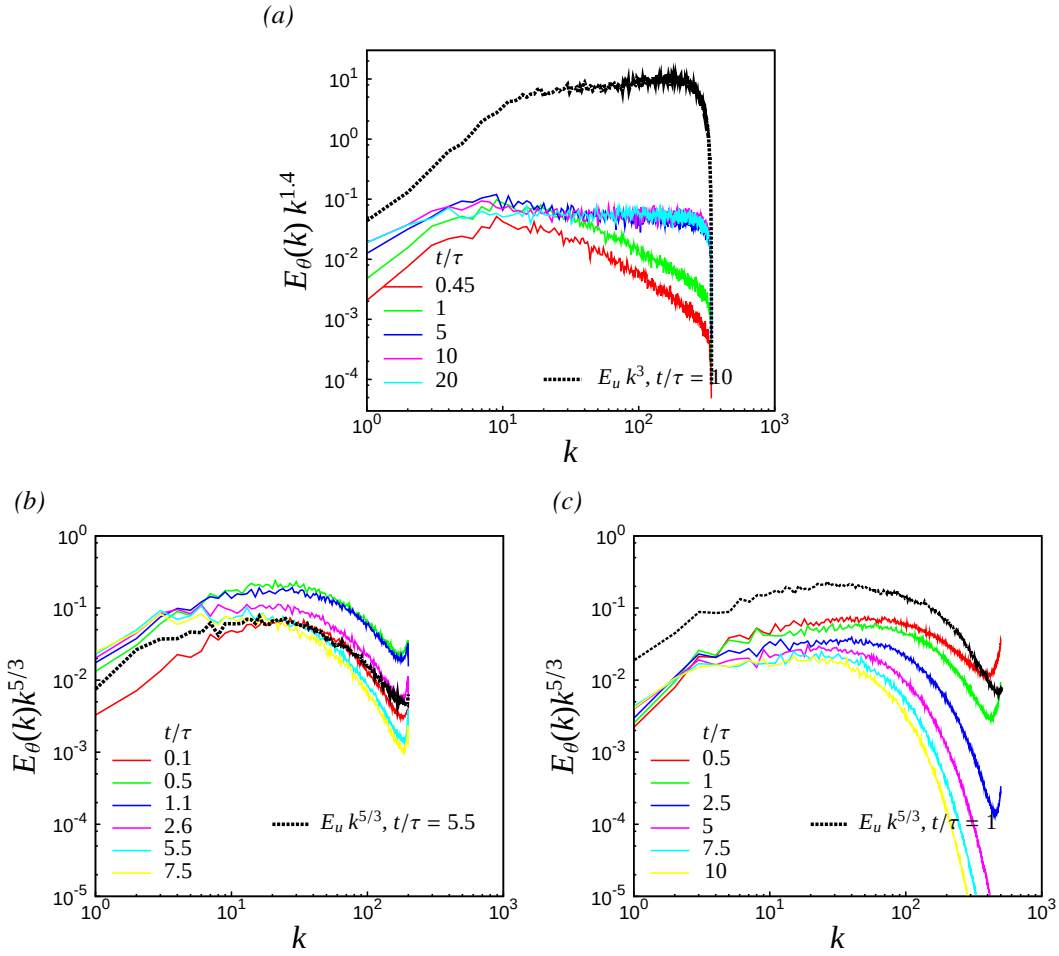

Figure 5: Compensated passive scalar one-dimensional spectra in the centre of the mixing layer in two (part a) and three dimensions at $Re_\lambda = 150$ (part b) and 250 (part c). The black dashed lines reproduce, at one instant, the compensated one-dimensional velocity spectrum in the same position. All spectra have been computed by integrating over the homogeneous directions y_i. All the simulations have an initial energy ratio $E_1/E_2 = 6.7$

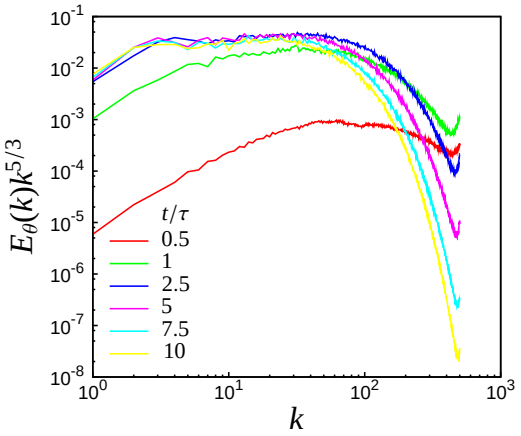

Figure 6: Compensated passive scalar one-dimensional spectra at $(x-x_c)/\ell(0) = 1.5$, where $\ell(0)$ is the initial integral scale, in the three dimensional mixing with $Re_\lambda = 250$ and energy ratio $E_1/E_2 = 6.7$. This position corresponds to about 1.5, 1.25, 0.5 and 0.25 observed values of $(x-x_c)/\Delta_\theta$ when t/τ is equal to 0, 1, 5 and 10, respectively.

Figure 6 shows the compensated spectra at 1.5 initial integral scale from the position of the initial interface, where the passive scalar gradient is zero at $t = 0$. In this position, the spectrum is reacher in small scales when this region is reached by the scalar fluctuations which propagates from the initial interface, then it gradually develops an inertial range as the scalar layer grows.

4 CONCLUSIONS

The spreading of a passive scalar interface in a shearless flow generates a region with a mean scalar gradient and a high scalar variance whose thickness shows a power law growth with exponents close to the ones of the turbulent energy diffusion length of the velocity field. The growth is faster in two dimensions, where it is superdiffusive while in three dimensions the exponent is close to 0.5. The passive scalar variance in the centre of the mixed layer is 50% higher in two dimensional case.

An important result concerns the generation of two passive scalar intermittent fronts which appear at the border of the mixed region which replaces the initial interface. The intermittency levels of the fronts is high and gradually decay in time. These fronts are generated close to the initial interface and then move toward the two homogeneous regions. Their displacement follows the growth of the thickness of the mixing region. However, they are not symmetric: the front toward the high energy side of the mixing penetrates deeper into it. This asymmetry is mild in the three-dimensional flow but is much pronounced in the two-dimensional flow, where the intermittency decays more slowly.

In the centre of the mixing layer, where the scalar variance has its maximum, both the the passive scalar and velocity spectra develop an inertial scaling range after about one initial eddy turnover time. In three dimensions, an exponent close to $-5/3$ is observed for both spectra but the scalar spectrum has a broader inertial range region than the velocity spectrum, as it was already been observed in other flows at moderate Reynolds numbers. In two dimensions, the velocity shows a κ^{-3} inertial range, while the passive scalar shows a κ^α inertial range with α close to 1.4. This exponent is closer to the three dimensional $\kappa^{-5/3}$ scaling than to the two dimensional k^{-1} scaling, which should be observed when the passive scalar is advected by a homogeneous turbulent flow.

References

[1] Shraiman B.I. and Siggia E.D., "Scalar turbulence," *Nature* **405**, 639–646 (2000).

[2] Warhaft Z., "Passive scalar in turbulent flows," *Ann. Rev. Fluid Mech.* **32**, 203–240 (2000).

[3] Tordella D. and Iovieno M., "Numerical experiments on the intermediate asymptotics of the shear-free turbulent transport and diffusion," *J. Fluid Mech.* **549**, 429–441 (2006).

[4] Tordella D., Iovieno M. and Bailey P.R., "Sufficient condition for Gaussian departure in turbulence," *Phys. Rev. E* **77**, 016309 (2008).

[5] Iovieno M., Tordella D., and Cavazzoni C., "A new technique for a parallel dealiased pseudospectral Navier-Stokes code," *Comp. Phys. Comm.* **141**, 365–374 (2001).

[6] Tordella D., Iovieno M., and Ducasse L., "Dimensionality influence on passive scalar transport," *Journal of Physics: Conference Series* **318**, 052042 (Proceedings of the 13th European Turbulence Conference), Warszawa, Poland, (2011).

[7] Veeravalli S., and Warhaft Z., "The shearless turbulence mixing layer," *J. Fluid Mech.* **207**, 191–229 (1989).

[8] Veeravalli S., and Warhaft Z., "Thermal dispersion from a line source in the shearless turbulence mixing layer," *J. Fluid Mech.* **216**, 35–70 (1990).

[9] Tordella D. and Iovieno M., "Small scale anisotropy in the turbulent shearless mixings," *Phys. Rev. Lett.* **107**, 194501 (2011).

[10] Danaila L., and Antonia R.A., "Spectrum of a passive scalar in moderate Reynolds number homogeneous isotropic turbulence," *Phys. Fluids.* **21**, 111702 (2009).

[11] Lee S.K., Benaissa A., Djenidi L., Lavoie P., and Antonia R.A.,"Scaling range of velocity and passive scalar spectra in grid turbulence," *Phys. Fluids.* **24**, 074101 (2012).

[12] Bos W.J., Kadoch B., Schneider K., Bertoglio J.P., "Inertial range scaling of the scalar flux spectrum in two-dimensional turbulence," *Phys. Fluids* **21**, 115105 (2009).

[13] Donzis D.A., and Yeung P.K., "Resolution effects and scaling in numerical simulations of passive scalar mixing in turbulence," *Physica D* **239**, 1287 (2010).

[14] Gotoh T., Nagaki J., and Kaneda Y., "Passive scalar spectrum in the viscous-convective range in two-dimensional steady turbulence," *Phys. Fluids* **12**, 155-168 (2000).

[15] Schumacher J., and Sreenivasan K.R., "Statistics and geometry of passive scalars in turbulence," *Phys. Fluids* **17**, 1–19 (2005).

[16] Emran M.S., and Schumacher J., "Fine-scale statistics of temperature and its derivatives in convective," *J. Fluid Mech.* **611**, 13–34 (2008).

[17] Gotoh T., and Watanabe T., "Scalar flux spectrum in isotropic steady turbulence with a uniform mean gradient", *Phys. Fluids* **19**, 121701 (2007).

[18] Zhou T., Antonia R.A., and Chua L.P., "Performance of a probe for measuring turbulent energy and temperature dissipation rates", *Exp. Fluids*, **33**, 334–345, (2002).